

## Noise-enhanced stability of sine-Gordon breathers

D. DE SANTIS<sup>(1)(\*)</sup>, C. GUARCELLO<sup>(2)(3)</sup>, B. SPAGNOLO<sup>(1)(4)</sup>, A. CAROLLO<sup>(1)</sup>  
and D. VALENTI<sup>(1)</sup>

<sup>(1)</sup> *Dipartimento di Fisica e Chimica “E. Segrè”, Group of Interdisciplinary Theoretical Physics, Università degli Studi di Palermo - I-90128 Palermo, Italy*

<sup>(2)</sup> *Dipartimento di Fisica “E. R. Caianiello”, Università degli Studi di Salerno I-84084 Fisciano, Salerno, Italy*

<sup>(3)</sup> *INFN, Sezione di Napoli, Gruppo Collegato di Salerno - Complesso Universitario di Monte S. Angelo, I-80126 Napoli, Italy*

<sup>(4)</sup> *Radiophysics Department, Lobachevsky State University - 603950 Nizhniy Novgorod, Russia*

received 26 January 2023

**Summary.** — A noise-induced enhancement of the breather stability in a lossy, stochastic sine-Gordon system is discussed. The numerical solutions indicate that a spatially uniform noisy source enables a stationary breather to survive way beyond its deterministic lifetime. An average characteristic time for the breather is defined, whose values vary nonmonotonically as a function of the noise strength, while being almost unaffected by the mode’s initial phase.

### 1. – Introduction

The combination of nonlinearity and noise can lead to surprising phenomena. Prominent examples are stochastic resonance [1], stochastic resonant activation [2], and noise-enhanced stability (NES) [2-6]. In the latter case, the stability of an unstable system increases thanks to a finite noise strength —definitely a counterintuitive fact. Starting from the pioneering work in ref. [3], the NES effect has attracted a great deal of interest across the scientific community [2, 4-6].

Here, the stability of breather solutions of the sine-Gordon (SG) equation [7, 8] is considered. An SG breather is a space-localized, time-periodic soliton formed by two elementary SG excitations with opposite topological charge, *i.e.*, by a kink and an antikink [7, 8].

The focus on the SG framework is motivated by the wide range of both purely physical and interdisciplinary applications in, *e.g.*, gravity and black holes [8], seismology [9], biophysics [10], superconductor-based systems [11], and Bose-Einstein condensates [12]. In particular, the experimental observation of breathers in long Josephson junctions (LJJs) [11] is a long-established problem in mesoscopic soliton physics [13-17], and its resolution requires a detailed understanding of the stochastic dynamics of these nonlinear excitations. Moreover, both optically-excited breathers in cuprate superconductors [11] and breather-type oscillations of the global tectonic shear stress fields [18]

(\*) E-mail: [duilio.desantis@unipa.it](mailto:duilio.desantis@unipa.it)

have been detected in the last few years. Note also that breather modes are actively studied even beyond the SG model as well as in discrete systems [19].

An important issue concerning SG breathers is that, when friction comes into play, they are unstable [20]. Inspired by recent investigations showing that noise can have beneficial effects in the generation of breather states [13-17], a noisy SG equation is examined below in the presence of dissipation to establish whether the stochastic term can positively affect the persistence time of these solitonic excitations. Interestingly, the simulations reveal that a spatially uniform noisy source allows a stationary breather to survive way past its lifetime in the purely dissipative (deterministic) case. An average characteristic time for the breather is defined, whose behaviour is nonmonotonic as a function of the noise strength. Different values of the mode's initial phase are chosen, and the results are very close to each other.

## 2. – The model

Equation

$$(1) \quad \varphi_{xx} - \varphi_{tt} - \alpha\varphi_t = \sin \varphi - \gamma(t)$$

is considered for the field  $\varphi(x, t)$  over the region  $[-l/2, l/2] \times [0, t_{\text{obs}}]$ , with  $l = 50$  and  $t_{\text{obs}} = 250$  being the system length and the observation time, respectively. In eq. (1), partial differentiation is indicated via subscripts,  $\alpha = 0.02$  is a friction coefficient, and  $\gamma(t)$  is a spatially-uniform, Gaussian stochastic force with zero average and autocorrelation function  $\langle \gamma(t_1)\gamma(t_2) \rangle = 2\Gamma\delta(t_1 - t_2)$ .

Equation (1) is numerically integrated with the boundary conditions  $\varphi_x(-l/2, t) = \varphi_x(l/2, t) = 0$  and the initial conditions  $\varphi(x, 0) = \varphi^b(x, 0)$  and  $\varphi_t(x, 0) = \varphi_t^b(x, 0)$ , where

$$(2) \quad \varphi^b(x, t) = 4 \arctan \left[ \frac{\sqrt{1 - \omega^2}}{\omega} \frac{\sin(\omega t + \vartheta)}{\cosh(\sqrt{1 - \omega^2}x)} \right]$$

is the stationary breather solution of the pure SG equation, *i.e.*, eq. (1) with  $\alpha = \gamma(t) = 0$ , in an infinite spatial domain [7, 8]. In eq. (2),  $\omega = 0.9 < 1$  and  $0 \leq \vartheta \leq 2\pi$  are the oscillation frequency and phase, respectively.

Note that the above framework reliably models the behavior of an overlap LJJ, in the absence of external magnetic fields, when the friction and a randomly-varying electrical bias are taken into account [11]. In this case, space and time are normalized to the Josephson penetration depth  $\lambda_J$  and the inverse of the Josephson plasma frequency  $\omega_p$ , respectively [11]. The initial condition corresponds to a stationary breather being generated at the LJJ's midpoint. Actually, the Josephson realm provides a solid physical background for this study, and the parameters are fixed to values typical in such a context [13-17].

From a numerical standpoint, the SG system is handled via an implicit finite-difference scheme, with discretization steps  $\Delta x = \Delta t = 0.005$ , see ref. [21] for further details.

## 3. – Results and discussion

In the presence of both dissipation and noise, two main “decay channels” can be identified: i) a kink-antikink pair arises due to the energy gain from the stochastic fluctuations (fig. 1(a)); ii) the breather relaxes into radiative modes (fig. 1(b)).

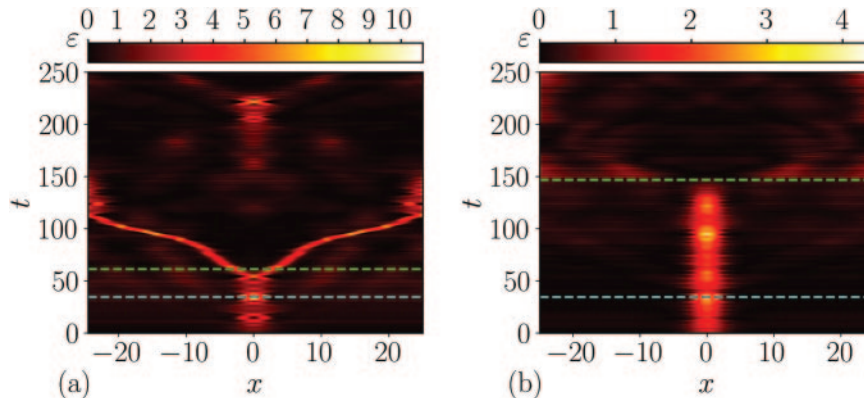


Fig. 1. – Energy density,  $\varepsilon(x, t) = 0.5(\varphi_t^2 + \varphi_x^2) + 1 - \cos \varphi$  [7, 8], for two different realizations. In panel (a), where  $\Gamma = 10^{-2}$  and  $\vartheta = 0$ , a kink-antikink splitting can be appreciated at  $t = \tau \approx 65$ . In panel (b), where  $\Gamma = 7 \times 10^{-3}$  and  $\vartheta = 0$ , a radiative decay scenario is illustrated for a breather which persists up to  $t = \tau \approx 150$ . In panel (a) (panel (b)), the cyan and green dashed horizontal lines denote the deterministic breather lifetime, *i.e.*,  $\ln(2)/\alpha \approx 35$ , and the instant  $t = \tau \approx 65$  ( $t = \tau \approx 150$ ), respectively.

Since no  $x$ -dependent perturbations are included in eq. (1), the evolution of the stationary breather can be followed by monitoring its oscillation center, namely  $x = 0$ . In particular, in view of the two scenarios described above, for each run,  $\tau_{2\pi}$  and  $\tau_{1/2}$  are defined as the smallest time instants at which the breather's amplitude reaches values  $2\pi$  and  $\varphi_{1/2}^b = 2 \arctan(\sqrt{1 - \omega^2}/\omega)$ , respectively. In the former case, the hitting of  $2\pi$  signals the emergence of kink-type structures, whereas in the latter case, the halving of the excitation's amplitude with respect to its initial value (see eq. (2)) is reasonably related to substantial radiative losses. The quantity  $\tau = \min\{\tau_{2\pi}, \tau_{1/2}\}$ <sup>(1)</sup> is then introduced, and it represents a proxy of the breather's lifetime in the presence of noise (see, *e.g.*, the green dashed horizontal lines in fig. 1) [21].

With  $\tau(\Gamma = 0) \approx \ln(2)/\alpha$  serving as the reference point, fig. 2 illustrates the relative change of the average characteristic time  $\langle \tau \rangle$ , computed over  $N = 2500$  realizations, versus the noise amplitude  $\Gamma \in [10^{-5}, 10^{-2}]$ . Here, four initial phase values  $\vartheta$  are examined (black circles,  $\vartheta = 0$ ; red squares,  $\vartheta = \pi/2$ ; green triangles,  $\vartheta = \pi$ ; blue diamonds,  $\vartheta = 3\pi/2$ ). Firstly, the plot highlights, regardless of  $\vartheta$ , the robustness of the breather against noise, *i.e.*,  $\langle \tau \rangle \approx \tau(\Gamma = 0)$  is observed for a significant range of amplitudes  $\Gamma$ . Figure 2 also displays closely spaced nonmonotonic trends for the different  $\vartheta$  values, *i.e.*, evidence of a positive noise-induced effect on the breather's stability is found.

This interesting phenomenon is exemplified in fig. 1 for  $\vartheta = 0$ . In particular, the strongly localized mode is seen to survive up to  $t = \tau \approx 150$  in fig. 1(b) (see the green dashed horizontal line), *i.e.*, far beyond its deterministic lifetime, thanks to the noisy force's energy input.

In conclusion, this paper shows that a spatially-uniform noise source can be beneficial for the SG breather's persistence, independently of the initial phase  $\vartheta$ . Noise can thus

<sup>(1)</sup> This expression holds when both  $\tau_{2\pi}$  and  $\tau_{1/2}$  can be evaluated. If, in a given run, only  $\tau_{2\pi}$  ( $\tau_{1/2}$ ) is defined, one simply considers  $\tau = \tau_{2\pi}$  ( $\tau = \tau_{1/2}$ ).

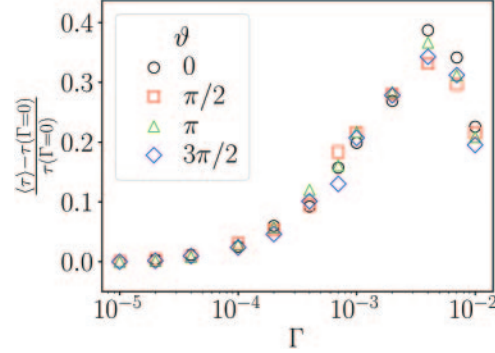


Fig. 2. – Relative change of the quantity  $\langle \tau \rangle$ , computed over  $N = 2500$  realizations, *vs.* the noise strength  $\Gamma \in [10^{-5}, 10^{-2}]$ . Each of the different marker types corresponds to a phase value  $\vartheta$ : black circles,  $\vartheta = 0$ ; red squares,  $\vartheta = \pi/2$ ; green triangles,  $\vartheta = \pi$ ; blue diamonds,  $\vartheta = 3\pi/2$ .

represent a control parameter within an experimental setup devoted to the breather's detection and related applications [13-17]. See ref. [21] for more information.

\* \* \*

This work was supported by the Italian Ministry of University and Research (MUR).

## REFERENCES

- [1] BENZI R. *et al.*, *J. Phys. A*, **14** (1981) L453.
- [2] GUARCELLO C. *et al.*, *Phys. Rev. B*, **92** (2015) 174519; GUARCELLO C. *et al.*, *J. Stat. Mech.: Theory Exp.*, **2016** (2016) 054012; SPAGNOLO B. *et al.*, *Entropy*, **19** (2017) 20.
- [3] MANTEGNA R. N. and SPAGNOLO B., *Phys. Rev. Lett.*, **76** (1996) 563.
- [4] SPAGNOLO B. *et al.*, *Acta Phys. Pol. B*, **38** (2007) 1925.
- [5] GUARCELLO C., *Chaos, Solitons Fractals*, **153** (2021) 111531.
- [6] GUARCELLO C. *et al.*, *Acta Phys. Pol. B*, **44** (2013) 997.
- [7] SCOTT A. C., *Nonlinear Science* (Oxford University Press) 2003.
- [8] CUEVAS J. *et al.* (Editors), *The sine-Gordon Model and its Applications* (Springer) 2014.
- [9] BYKOV V. G., *J. Seismol.*, **18** (2014) 497.
- [10] PEYRARD M. (Editor), *Nonlinear Excitations in Biomolecules* (Springer) 1995.
- [11] BARONE A. and PATERNÒ G., *Physics and Applications of the Josephson Effect* (Wiley) 1982; DIENST A. *et al.*, *Nat. Mater.*, **12** (2013) 535.
- [12] SU S.-W. *et al.*, *Phys. Rev. A*, **91** (2015) 023631.
- [13] DE SANTIS D. *et al.*, *Chaos, Solitons Fractals*, **158** (2022) 112039.
- [14] DE SANTIS D. *et al.*, *Commun. Nonlinear Sci. Numer. Simul.*, **115** (2022) 106736.
- [15] DE SANTIS D. *et al.*, *Nuovo Cimento C*, **45** (2022) 166.
- [16] DE SANTIS D. *et al.*, *Chaos Solitons Fractals*, **170** (2023) 113382.
- [17] DE SANTIS D. *et al.*, arXiv:2306.13338 (2023).
- [18] ŽALOHAR J. *et al.*, *J. Struct. Geol.*, **140** (2020) 104185.
- [19] LIAZHKOVA S. D., arXiv:2212.09441 (2022).
- [20] MCLAUGHLIN D. W. and SCOTT A. C., *Phys. Rev. A*, **18** (1978) 1652.
- [21] DE SANTIS D. *et al.*, *Chaos, Solitons Fractals*, **168** (2023) 113115.